IEEE Photonics Journal
An IEEE Photonics Society Publication

Open Access

Rapid Evaluation of All-Optical Modulation in Quantum Cascade Laser Using Photoluminescence Spectrum

Volume 10, Number 4, August 2018

Haijun Zhou
Chen Peng
Liguo Zhu
Tao Chen
Yuankun Sun
Gang Chen
Zeren Li
Qixian Peng
Peng Feng
Biao Wei

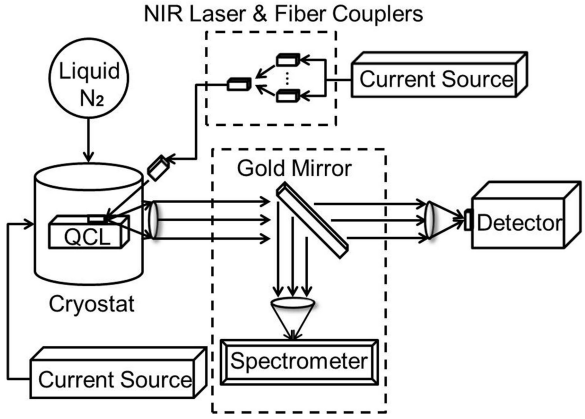

DOI: 10.1109/JPHOT.2018.2859823
1943-0655

IEEE photonics SOCIETY

IEEE

Rapid Evaluation of All-Optical Modulation in Quantum Cascade Laser Using Photoluminescence Spectrum

Haijun Zhou,[1] **Chen Peng**,[2] **Liguo Zhu**,[2] **Tao Chen**,[2] **Yuankun Sun**,[1,2] **Gang Chen**,[1] **Zeren Li**,[2] **Qixian Peng**,[2] **Peng Feng**,[1] **and Biao Wei**[1]

[1]Key Laboratory of Optoelectronic Technology and Systems, Ministry of Education, Chongqing University, Chongqing 400044, China
[2]Institute of Fluid Physics, China Academy of Engineering Physics, Mianyang 621900, China

DOI:10.1109/JPHOT.2018.2859823

Manuscript received June 12, 2018; accepted July 12, 2018. Date of publication July 25, 2018; date of current version August 10, 2018. This work was supported in part by the China Post-Doctoral Science Foundation under Grant 2018M633408, and in part by the National Natural Science Foundation of China under Grants 61177093 and 61077057. Haijun Zhou and Chen Peng contributed equally to this work. Corresponding author: Chen Peng (e-mail: pengchen1202@cqu.edu.cn).

Abstract: All-optical modulation in a quantum cascade laser (QCL) can be rapidly evaluated using a photoluminescence (PL) spectrum. The PL spectrum reflects the electron transition rate of the sub-bands of the active region of a QCL. The peak position, amplitude, and displacement of the PL spectrum can be used to determine the optimal wavelength, spot position, the laser incident angle, optical power, and displacement in the electric field of the near-infrared laser. This PL spectrum approach is rapid, accurate, and simple. Furthermore, it can be used to optimize high-speed all-optical modulation of QCLs for use in free-space optical communication and molecular-detection applications.

Index Terms: Luminescence and fluorescence, spectroscopy, quantum cascade laser.

1. Introduction

Mid-infrared lasers are widely used in free-space optical communications (FSOC) [1], [2] and molecular detection [3], [4] because of their advantages of covering atmospheric windows and molecular fingerprints. QCLs [5] are a promising mid-infrared coherent light source, which have the advantages of narrow line width, high power, and room-temperature operation; in addition, they are unipolar devices, which are conducive to high-speed all-optical modulation. The development of efficient modulation approaches [6], [7] for FSOC and molecular detection is of interest for an increasing number of applications. Compared to thermal and electric modulation, in all-optical modulation, the modulation frequency can be greatly improved up to 100 GHz [8]. Recently, the high-speed all-optical modulation of QCLs has resulted in corresponding progress in QCL applications [9]–[12]. The conventional all-optical modulation system of QCLs is realized by using a NIR to illuminate the QCLs [13]. However, in the experiment, we confirm that the optimal conditions of all-optical modulation in QCL are a complex debugging process. Further, the NIR wavelength, spot position, the laser incident angle, and optical power considerably affect all-optical modulation. At present, there is no report on the rapid evaluation of all-optical modulation in QCL, and it depends

on previous experiments and experimenters' experience. In this study, we propose an approach for rapidly evaluating the all-optical modulation of QCLs using a PL spectrum. The proposed approach can determine the modulation parameters rapidly, simplify the experimental system, and obtain the optimal NIR wavelength directly.

High-speed all-optical modulation of QCLs depends on the excitation of external light, which makes the electrons in the QCL active region transition from the valence band to the conduction band. This process results in a change in the electronic distribution, and this ultimately leads to the modulation of the QCL output. Further, as the electron distribution affects the refractive index of the QCL [6], the QCL output wavelength is also modulated to achieve frequency modulation. Amplitude and frequency modulation with the all-optical approach proceed with a high speed because the electron relaxation time is usually only about 1–100 ps [14]. The all-optical modulation of QCL requires the external laser excitation energy to be greater than the band gap of the QCL active region. The band gap depends on the material and the n-doping of the quantum well and the barrier, and it can be obtained through numerical calculations. Previous studies have shown that excessive external laser excitation energy generates hot carriers [15], which reduce the modulation effect [16]. In order to obtain the optimal wavelength of the modulated laser, it is usually necessary to use different external lasers for the test separately. The PL is generated owing to the transition of the excited electrons from the conduction band to the valence band. So the PL spectrum can rapidly finds the highest electron transition rate of the sub-bands, which can guide us to find the optimal wavelength of all optical modulation rapidly. Moreover, PL spectrum is weak and sensitive to the NIR wavelength, spot position, the laser incident angle, and optical power, and is conducive to simultaneous optimization of parameters. And the PL spectrum can be obtained by switching a golden mirror in the all-optical modulation system, which will not affect the normal operation of the all-optical modulation system. Therefore, we using PL spectrum to evaluation of all-optical modulation in QCL rapidly.

2. Simulation

A numerical approach was also employed to study the energy levels and wave functions of QCLs. This simulation is based on our model of QCL output characteristics, [17] which includes stimulated emission, spontaneous emission, and the sub-band electron temperature effect. The initial energy level and wave functions in the quantum well structure are determined using Schrödinger's equation [18]. To solve full rate equations, we obtained the electron population of all sub-bands and photon populations, and we corrected the energy levels and wave functions. Then, we used the sub-band electron temperature effect on a QCL to calculate the new electron population and scattering rate for obtaining the final correction of the energy levels and wave functions. In this simulation, the laser is a standard 35-stage $In_{0.52}Al_{0.48}As$/ $In_{0.52}Ga_{0.47}As$ type-I four-level Fabry-Perot QCL based on a two-phonon resonant design [19]. Figure 1 shows the calculated electrical potential and the electron spatial probability distribution for each sub-band in the active region and two injection regions, for a bias electrical field of 50 kV/cm. The active region is sandwiched between the two injection regions. There are seven confined sub-bands in each region, and sub-bands A_i, I_i, and I'_i for the active region and injection regions, respectively. For the two laser sub-bands A_3 and A_4, the band gap difference is 0.159 eV, which corresponds to the QCL's central wavelength of 7.81 μm. A wavelength range of NIR laser can achieve all-optical modulation, and the wavelength range is corresponding to the simulation results. So this simulation can provide guidance for the next experiment. But in fact, the wavelength of NIR laser corresponding to the upper laser level of is not necessarily the optimal wavelength. However, the influence of parameters such as spot position, incident angle on all-optical modulation is difficult to get accurately by numerical calculation. And the PL spectrum can accurately and rapidly evaluate all parameters. In addition, the all-optical modulation is not only determined by the pump photon energy [6], but also the hot carrier effect has played a significant role [20]. So the numerical calculation is impossible to replace the PL spectrum experiment in evaluate all-optical modulation of QCL.

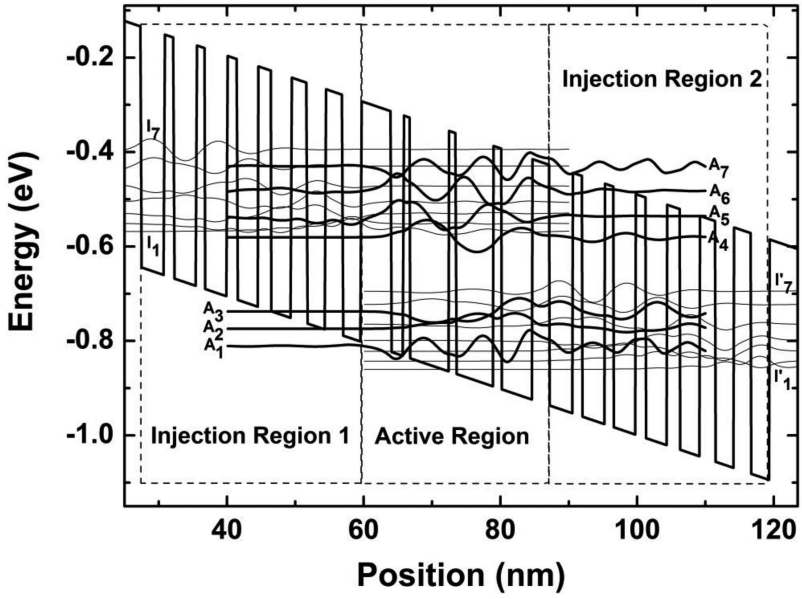

Fig. 1. Calculated conduction sub-bands and the moduli squared of the relevant wave functions at a 50 kV/cm DC bias.

3. Experimental Results

Figure 2 shows the schematic diagram of the experimental setup. The QCL was mounted on a copper heat sink inside a liquid nitrogen cryostat (Janis VPF) and held at a temperature of 80 K; we utilized a current source (ILX Lightwave LDP 3811) to drive the QCL. Using two CaF_2 lenses, the QCL's MIR emission is collimated and then focused onto an infrared photovoltaic detector (Vigo PEMI-2TE-6). A reversible gold mirror is used to transmit the PL onto a spectrometer. The NIR beams are focused on the QCL front facet with an incident angle about 20°–90° to the QCL beam, and the NIR focal spot diameter is less than 20 μm. Fast and convenient replacement of NIR lasers with different wavelengths is achieved by using fiber couplers.

In the all-optical modulation of QCLs, the NIR laser wavelength directly affects the modulation depth; therefore, we need to choose an optimal wavelength of the NIR laser. We use the external light to excite QCLs to generate PL in order to rapidly evaluate the electron transition rate in the sub-bands. According to the simulation results, each sub-band has the different electron transition rates. To cover all sub-bands, the energy of the NIR laser must be greater than the widest band gap (1.45 eV) of the QCL. We use a Ti: sapphire laser with a wavelength of 840 nm ($<$857 nm, corresponding 1.45 eV) to illuminate the front facet of the QCL. In order to protect the QCL, the average power of the Ti: sapphire laser is set to be less than 3 mW before the Dewar window. As show in Figure 3, we normalize the spectrum signals, and the Ti: sapphire laser spectrum peak is at 840 nm and the PL spectrum has two distinct peaks. One PL spectrum peak is at 1.55 μm. This PL peak is produced by the electron transition from the laser sub-bands A_3 and A_2, A1 to the valence band, and it has the highest electron transition rate. At the same time, another PL spectrum peak is at 1.36 μm. It is produced by the electron transition from the laser sub-band A_4 to the valence band, and it has a lower transition rate. The electron transition rate for other sub-bands is lower, because there is no corresponding PL spectrum. According to the experimental results of PL spectrum, the NIR laser wavelength corresponding to the highest electron transition rate of the sub-bands is 1360 nm and 1560 nm. 1360 nm and 1560 nm are identified as the optimal NIR laser wavelengths. In order to ensure the correctness of the experiment, we tested the entire wavelength range corresponding to the simulation. According to our existing experimental

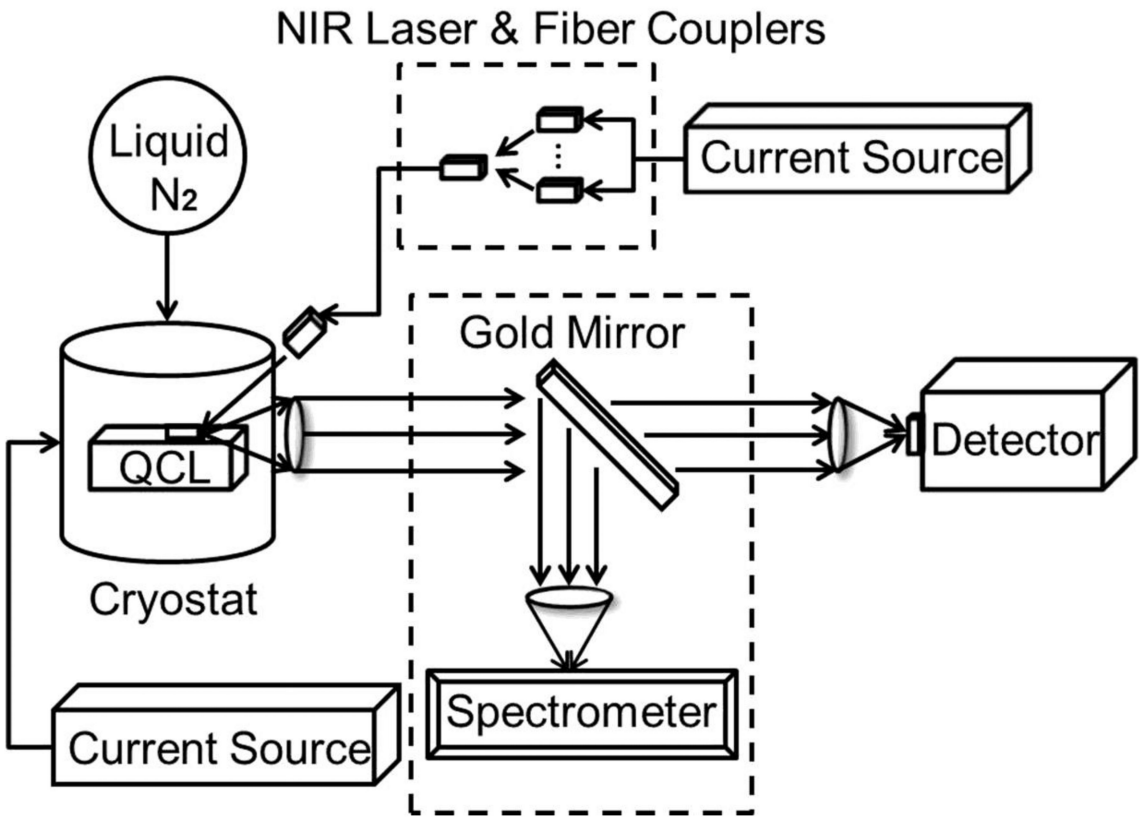

Fig. 2. Experiment setup for evaluating the all-optical modulation of a quantum cascade laser using photoluminescence spectrum.

conditions, we use eleven different NIR lasers emitting at wavelengths of 850, 905, 980, 1280, 1310, 1360,1450,1550,1560, 1570 and 1590 nm to excite the QCL for proving this conclusion. The short wavelength lasers (850, 905, and 980 nm) lead to a reduction in QCL intensity, and the long wavelength lasers (1280–1590 nm) lead to an increasing in QCL intensity. As shown in the inset in Figure 3, The QCL modulation depth are 11.32%, 13.72%, 14.18%, 14.65%, 17.31%, 17.86%, 17.73%, and 16.81%, respectively. The experiment results show that 1560 nm NIR lasers have the maximum modulation depth of QCL, which is 17.86%, while the 1360 nm NIR laser has not the second high QCL modulation depth, which is only 14.18%. Further, we used 1550 nm and 1570 nm NIR lasers to confirm the QCL modulation depth around 1560 nm. Experimental results show that both 1550 nm and 1570 nm have high QCL modulation depth, but lower than 1560 nm. So we can confirm that 1560 nm is the optimal NIR laser wavelength. With the increase of the NIR laser wavelength, the NIR laser not only affects the electron interband transition in the upper and lower laser levels, but the electron interband transition of other sub-bands is also involved, so the higher modulation depth is obtained. It is sufficient to prove that using the PL spectrum to evaluate the optimized wavelength of the NIR laser in the QCL all-optical modulation is a reliable method.

Compared to thermal and electrical modulation, the NIR laser-spot position has a considerable influence on all-optical modulation of QCLs. To achieve a higher modulation depth of QCLs, the electron transitions of QCL require more optical energy. The QCL's core region is usually between the top contact and the substrate, only about 100–200 μm. It is difficult to obtain high modulation efficiency if the optimal NIR laser-spot position cannot be determined. If the spot position is not determined, the optical energy cannot effectively inject the core region of the QCL to change the

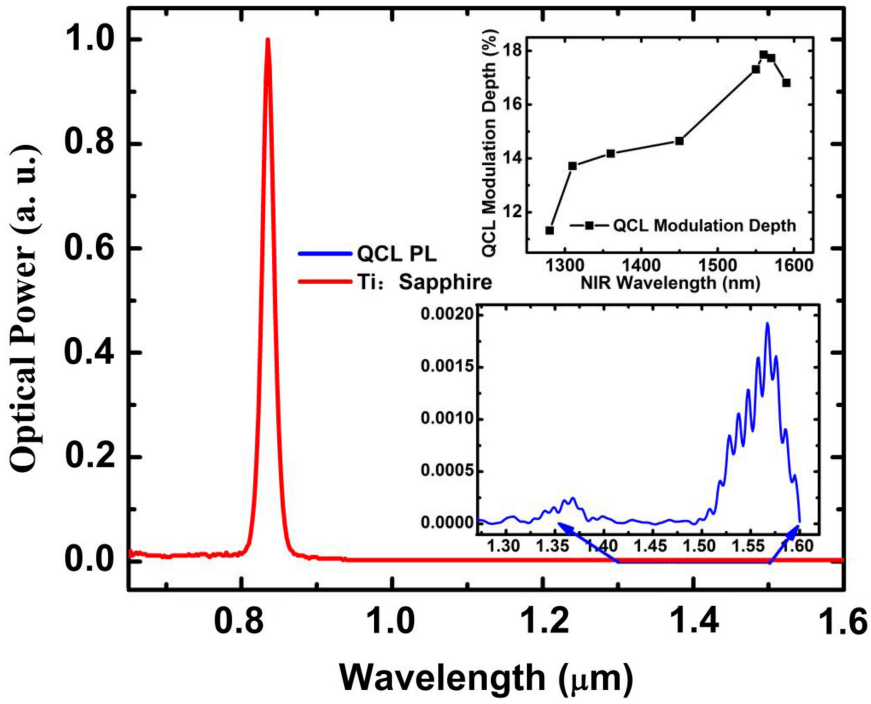

Fig. 3. The Ti: Sapphire laser spectrum with a wavelength of 840 nm; the inset shows the PL spectrum of QCL excited with the Ti: Sapphire laser and the QCL modulation depth excited by long wavelength NIR lasers.

carrier's distribution, and then they will increase the temperature of the QCL through the heat accumulation, and then cause the QCL to be damaged. In the PL spectrum experiment, the diameter of the NIR laser spot is generally less than 20 μm, and the average power is low. In this experiment, we use a semiconductor laser with a wavelength of 1560 nm to illuminate the front facet of the QCL, and the diameter of the spot is about 20 μm. We switch the spot vertical position of the NIR laser in the QCL core region and observe the PL spectrum. As shown in Figure 4, there are PL spectrum at the spot vertical position of the NIR laser between 5.005 and 5.065 mm, and the strongest signal is at 5.045 mm (4.04×10^{-6} mW). We considering the diameter of the NIR laser spot, the range of the illuminating spot will be expanded. We obtain the optimal NIR laser spot within the range of 40 μm in the center of the QCL core region. The traditional method of observing the change of current and voltage of QCL has greater error. At the same time, we measure the QCL's current and voltage when the NIR laser spot vertical position is changed. As shown in the inset in Figure 4, the QCL voltage is reduced under NIR laser modulation, and the lowest voltage is -0.12 V at the spot vertical position of the NIR laser at 5.045 mm. In addition, the QCL current is increased under NIR laser modulation, and the highest current is 16 mA at the spot vertical position of the NIR laser at 5.06 mm (2.28×10^{-6} mW). With the same consideration of the diameter of the NIR laser spot, the error is about 70 μm. This is due to NIR laser modulation that makes the electrons of QCL transition from the valence band to the laser sub-band in the conduction band, thus generating a voltage, while reducing the required current. And with the increase of modulation efficiency, the phenomenon will be more obvious. But it is inevitable to introduce errors of evaluating the QCL modulation depend on observing the change of QCL voltage and current. Moreover, outside the region of about 60 μm at the spot vertical position of the NIR laser, the QCL voltage and current changes are negligible. In order to confirm the correctness of the PL spectrum, we simultaneously measure the QCL modulation depth at the same position. In

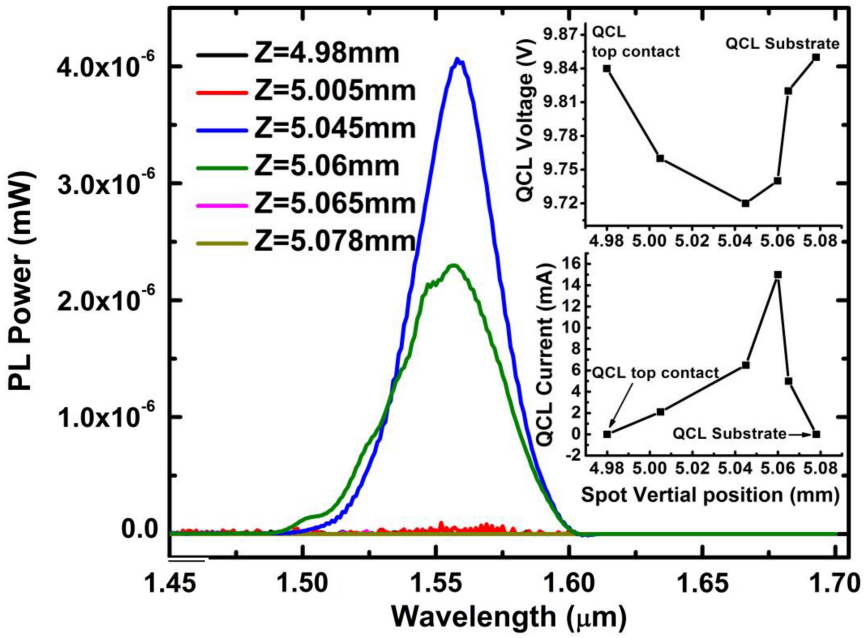

Fig. 4. The PL power at different NIR laser spot vertical positions; the inset shows the QCL current and QCL voltage under the NIR laser modulation at different spot vertical positions.

fact, all optical modulation is very sensitive to the spot position of the near infrared light. Only the modulation exists in 5.045 mm and 5.06 mm, and there is no modulation in other spot positions. The modulation depth at 5.045 mm is 17.86%, while the modulation depth at 5.06 mm is 9.62%. It is worth mentioning that the modulation depth ($17.86\% : 9.62\% = 1.86$) is proportional to the PL spectrum power (4.04×10^{-6} mW: 2.28×10^{-6} mW $= 1.77$), and this is impossible to use the method of the observing current and voltage changes. Therefore, So PL spectrum is obvious a guidance, we can further confirm the optimal position of the NIR laser spot.

In the QCL all-optical modulation, the optical energy injected into the QCL active region will directly affect the QCL modulation depth, which has been reflected in the research of spot position experiments. The NIR laser incident angle and optical power directly determine the optical energy of the QCL active region injected. In order to comprehensively investigate the effect of laser incident angle and optical power on the QCL modulation depth, we have measured at the same system and conditions. The NIR laser spot position at 5.045 mm, the NIR laser wavelength is 1560 nm, and the average power is 3 mW. The NIR laser is focused on QCL front facet, and the incident angle is 20°−90° from the vertical incident to the horizontal incident. As shown in the inset in Figure 5, to ensure that QCL MIR and PL are not obscured, we can measure the laser incident angle at 20°. As shown in Figure 5, with the increase of laser incident angle, the PL power decreases gradually. Especially when the laser incident angle increases to more than 60°, the PL power accelerates to decrease. When the laser incident angle is 90°, the PL power is only 0.7 nW. We also measured the corresponding QCL modulation depth, which is consistent with the variation of PL power. We can think that when the NIR laser is vertically incident QCL front facet, the QCL active region participates in the inter band transition energy, which causes the electron distribution of subband to change greatly, so the QCL modulation depth is large. With the increase of the laser incident angle, the optical energy component into the QCL active region is reduced. After the laser incident angle is greater than 60°, only a small amount of optical energy can be injected in the QCL active region. This result is also reflected in the PL power. It is proved that the influence of laser incident angle on QCL all-optical modulation can be accurately evaluated by using PL. In addition, we measured

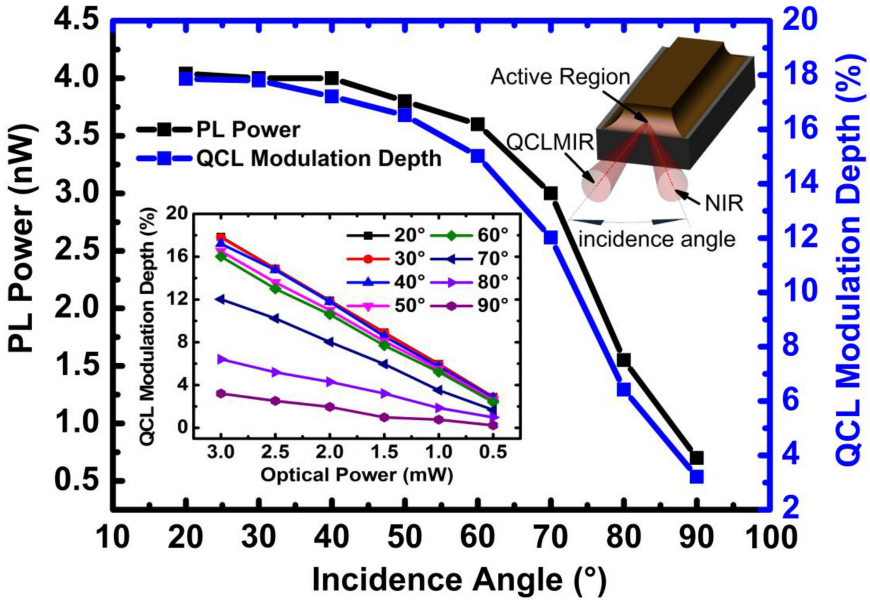

Fig. 5. The PL power and QCL modulation depth with different NIR laser incident angles; the inset shows the QCL modulation depth at different optical power and the cartoon of all-optical modulation on a QCL via front facet illumination with an external NIR laser.

the effect of optical power on the QCL modulation depth. We used the NIR laser with an average optical power of 0.5–3 mW and obtained the corresponding QCL modulation depth according to the variation of PL power. As shown in the inset in Figure 5, with the optical power decrease, the QCL modulation depth will also decrease. When the laser incident angle is less than 60°, the changing trend of QCL modulation depth is the same, but when the laser incident angle is larger than 60°, the QCL modulation depth decreases rapidly, even difficult to obtain at 0.5 mW. This is because the optical energy injected into the QCL active region decreases rapidly with the laser incident angle increase. When the optical power is reduced at the same time, there is less energy involved in the interband transition in the QCL active region, so it is difficult for QCL to be modulated.

In QCLs, as the electric field is increased, the bottom of the subbands increases in energy, relative to the center of the quantum well structure. Hence, the reference subbands energy increases. It is causing the electrons to make orientated motion, which makes the QCL generate optical radiation. However, in this process, the change of the subbands energy corresponding to the optimal modulation wavelength drift, which is usually weak and is difficult to measure by traditional means. Using the PL spectrum, we can accurately and rapidly confirm the drift of the optimal modulation wavelength. In this experiment, we load a 0–300 mA current for the QCL and measure the PL spectrum simultaneously. As shown in Figure 6, with an increase in the electric field, the position of the PL spectrum peak has been drifting obviously, from 1563.9 nm to 1554.8 nm. The corresponding optimal wavelength of the NIR laser also reduces by a total of 9.1 nm. For a further confirmation, we load a 300 mA current for the QCL, using 1550 nm and 1560 nm NIR laser to modulate the QCL and the modulation depth is 15.34% and 14.34% respectively. The optimal modulation wavelength can be close to 1550 nm, is1554.8 nm. Simultaneously, we can also determine the optimal modulation wavelength of QCL under the current of 5 mA, 10 mA, 50 mA, 100 mA, 200 mA, as shown in the inset in Figure 6, which are 1562.9 nm, 1561.9 nm, 1559.8 nm, 1557.9 nm, and 1556.5 nm, respectively. In this manner, we can rapidly evaluate the all-optical modulation of QCLs under different electric fields using the PL spectrum.

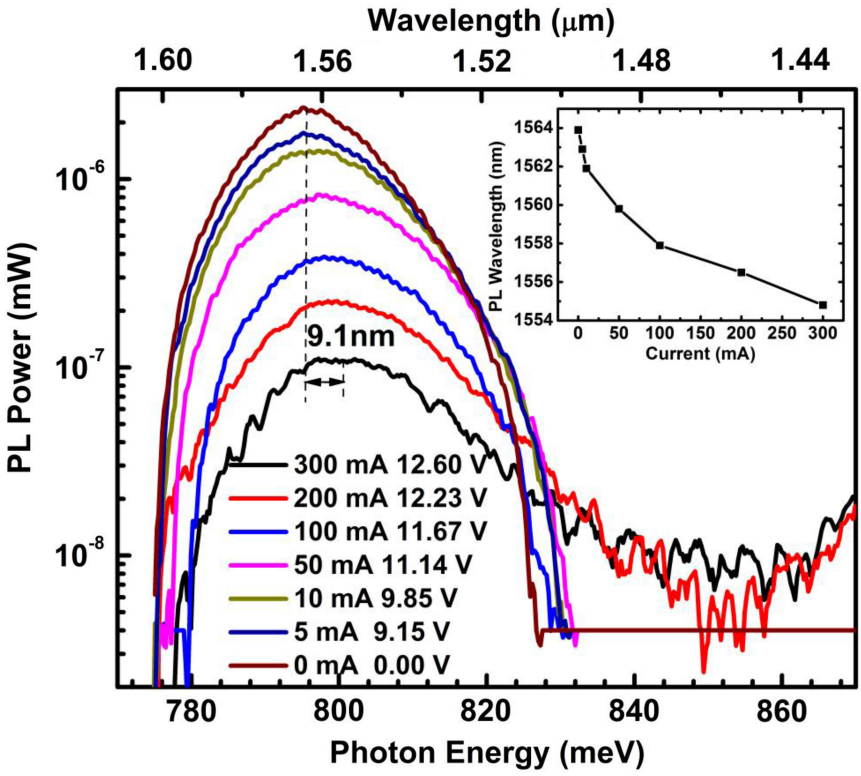

Fig. 6. The PL spectrum of QCL at different drive currents; the inset shows the PL spectrum peak at different drive currents.

4. Conclusions

In conclusion, using the PL spectrum to evaluate the all-optical modulation of QCLs is a novel approach. The optimal NIR laser wavelength can be confirmed by measuring the position of the PL spectrum peak, and the experimental results are in agreement with the simulation results. By measuring the intensity of the PL spectrum, we can confirm the NIR laser spot position accurately, and it is usually effective only in the range of tens of microns, and has considerable influence on the all-optical modulation of QCL. Meanwhile, we can also accurately identify the NIR laser incident angel and optical power by measuring the PL spectrum power. The optimization results can be directly applied to the experimental guidance. The displacement of the optimal NIR laser wavelength in the electric field can be accurately confirmed by measuring the position of the PL spectrum peak, which is usually difficult. Thus, the PL spectrum can be used to optimize the all-optical modulation of QCL, and it is rapid, accurate, and simple method. Thus, the high-speed all-optical modulation of QCLs can be optimized for FSOC and molecular detection applications.

Acknowledgment

The authors are grateful to OSA Publishing Language Editing Services for its linguistic assistance during the preparation of this Letter.

References

[1] R. Martini and E. A. Whittaker, "Quantum cascade laser-based free space optical communications," *J. Opt. Fiber Commun. Rep.*, vol. 2, no. 4, pp. 279–292, 2005.
[2] P. Corrigan, R. Martini, E. A. Whittaker, and C. Bethea, "Quantum cascade lasers and the -Kruse model in free space optical communication," *Opt. Exp.*, vol. 17, pp. 4355–4359, 2009.

[3] S. Welzel, G. Lombardi, P. B. Davies, R. Engeln, D. C. Schram, and J. Ropcke, "Trace gas measurements using optically resonant cavities and quantum cascade lasers operating at room temperature," *J. Appl. Phys.*, vol. 104, 2008, Art. no. 093115.
[4] S. Borri *et al.*, "Frequency modulation spectroscopy by means of quantum cascade laser," *Appl. Phys. B*, vol. 85, pp. 223–229, 2006.
[5] J. Faist, F. Capasso, D. L. Sivco, C. Sirtori, A. L. Hutchinson, and A. Y. Cho, "Quantum cascade laser," *Science*, vol. 264, pp. 553–556, 1994.
[6] G. Chen *et al.*, "Optically induced fast wavelength modulation in quantum cascade laser," *Appl. Phys. Lett.*, vol. 97, 2010, Art. no. 011102.
[7] S. Suchalkin, G. Belenlcy, and M. A. Belkin, "Rapidly tunable quantum cascade lasers," *IEEE J. Sel. Top. Quantum Electron.*, vol. 21, no. 6, Nov./Dec. 2015, Art. no. 1200509.
[8] F. Capasso, C. Gmachl, A. Tredicucci, A. L. Hutchinson, D. L. Sivco, and A. Y. Cho, "High performance quantum cascade laser," *Opt. Photon. News*, vol. 10, pp. 31–37, 1999.
[9] B. Hinlcov, A. Hugi, M. Beck, and J. Faist, "RF-modulation of mid-infrared distributed feedback quantum cascade lasers," *Opt. Exp.*, vol. 24, no. 4, pp. 3294–3312, 2016.
[10] X. D. Pang *et al.*, "Gigabit free-space multi-level signal transmission with a mid-infrared quantum cascade laser operating at room temperature," *Opt. Lett.*, vol. 42, no. 18, pp. 3646–3649, 2017.
[11] C. Peng *et al.*, "High-speed mid-infrared frequency modulation spectroscopy based on distributed-feedback quantum cascade laser," *IEEE Photon. Technol. Lett.*, vol. 28, no. 16, pp. 1727–1730, Aug. 2016.
[12] T. Stacewicz, Z. Bielecki, J. Wojtas, P. Magryta, J. Mikolagczyk, and D. Szabra, "Detection of disease makers in human breath with laser absorption spectroscopy," *Opto-Electron. Rev.*, vol. 24, no. 2, pp. 82–94, 2016.
[13] G. Chen, C. G. Beathe, and R. Martini, "Quantum cascade laser gain enhancement by front facet illumination," *Opt. Exp.*, vol. 17, pp. 24282–24287, 2009.
[14] C. Gmachl, F. Capasso, D. L. Sivco, and A. Y. Cho, "Recent progress in quantum cascade lasers and applications," *Rep. Prog. Phys.*, vol. 64, pp. 1533–1601, 2001.
[15] P. Harrison, D. Indjin, and R. W. Kelsall, "Electron temperature and mechanisms of hot carrier generation in quantum cascade laser," *J. Appl. Phys.*, vol. 92, pp. 6921–6923, 2002.
[16] T. Yang, G. Chen, C. Tian, and R. Martini, "Optical modulation of quantum cascade laser with optimized excitation wavelength," *Opt. Lett.*, vol. 38, pp. 1200–1202, 2013.
[17] C. Peng, G. Chen, T. Yang, S.-W. Park, and R. Martini, "Numerical study of subband electron temperature effect on a mid-infrared quantum cascade laser output characteristic," *Semicond. Sci. Technol.*, vol. 28, 2013, Art. no. 105008.
[18] R. Paiella, *Intersuband Transitions in Quantum Structures*. New York, NY, USA: McGraw-Hill, 2006.
[19] Z. J. Liu *et al.*, "Room-temperature continuous-wave quantum cascade lasers grown by MOCVD without lateral re-growth," *IEEE Photon. Technol. Lett.*, vol. 18, no. 12, pp. 1347–1349, Jun. 2006.
[20] C. Peng *et al.*, "Purified frequency modulation of a quantum cascade laser with an all-optical approach," *Opt. Lett.*, vol. 42, no. 21, pp. 4506–4509, 2017.